Spectroscopic and Biochemical Studies on Protein Variants of Quinaldine 4-Oxidase: Role of E736 in Catalysis and Effects of Serine Ligands on the FeSI and FeSII Clusters†

Reinhard Kappl,‡ Sonja Sielker,§ Kalina Ranguelova,‡ Jeannine Wegner,§ Katja Parschat,§ Jürgen Hüttermann,‡ and Susanne Fetzner*,§

Institut für Biophysik, Universität des Saarlandes, D-66421 Homburg, Germany, and Institut für Molekulare Mikrobiologie und Biotechnologie, Westfälische Wilhelms-Universität Münster, Corrensstrasse 3, D-48149 Münster, Germany

Received June 14, 2006; Revised Manuscript Received August 29, 2006

ABSTRACT: Quinaldine 4-oxidase (Qox), which catalyzes the hydroxylation of quinaldine to 1*H*-4-oxoquinaldine, is a heterotrimeric $(LMS)_2$ molybdo-iron/sulfur flavoprotein belonging to the xanthine oxidase family. Variants of Qox were generated by site-directed mutagenesis. Replacement in the large subunit at E736, which is presumed to be located close to the molybdenum, by aspartate (Qox_LE736D) resulted in a marked decrease in $k_{cat\ app}$ for quinaldine, while $K_{m\ app}$ was largely unaffected. Although a minor reduction of the glutamine substituted variant Qox_LE736Q by quinaldine occurred, its activity was below detection, indicating that the carboxylate group of E736 is crucial for catalysis. Replacement of cysteine ligands C40, C45, or C60 (FeSII) and of the C120 or C154 ligands to FeSI in the small subunit of Qox by serine led to decreased iron contents of the protein preparations. Substitutions C40S and C45S (Fe1 of FeSII) suppressed the characteristic FeSII EPR signals and significantly reduced catalytic activity. In Qox_SC154S (Fe1 of FeSI), the *g*-factor components of FeSI were drastically changed. In contrast, Qox proteins with substitutions of C48 and C60 (Fe2 of FeSII), and of the C120 ligand at Fe2 of FeSI, retained considerable activity and showed less pronounced changes in their EPR parameters. Taken together, the properties of the Qox variants suggest that Fe1 of both FeSI and FeSII are the reducible iron sites, whereas the Fe2 ions remain in the ferric state. The location of the reducible iron sites of FeSI and FeSII appears to be conserved in enzymes of the xanthine oxidase family.

The soil bacterium *Arthrobacter nitroguajacolicus* Rü61a (formerly assigned to the species *A. ilicis* (*1*)) utilizes quinaldine (2-methylquinoline) as sole source of carbon and energy (*2*, for a review, see ref *3*). The ability to grow on quinaldine is conferred by the linear conjugative plasmid pAL1, which seems to be widespread within the genus *Arthrobacter* (*1*). The degradation pathway starts with a hydroxylation of quinaldine in position 4, catalyzed by the inducible enzyme quinaldine 4-oxidase (Qox).[1] Qox shows exceptionally broad substrate specificity for various quinoline derivatives and benzodiazines and even catalyzes the oxidation of aromatic aldehydes (*4*). Remarkably, it converts quinoline and some derivatives as well as isoquinoline, quinazoline, and cinnoline with a significantly higher rate than quinaldine, suggesting imperfect adaptation of the enzyme to its physiological substrate.

Qox belongs to the xanthine oxidase (XO) family of mononuclear molybdenum enzymes, which catalyze the incorporation of an oxygen atom, derived from a water molecule, into a C−H bond of an *N*-heteroaromatic compound or an aldehyde. Oxidative hydroxylation takes place at the molybdenum center. Like most other bacterial molybdenum enzymes involved in the degradation of *N*-heteroaromatic substrates, Qox shows an $(LMS)_2$ subunit

† This work was supported by the Volkswagen Foundation within the priority programme "Intra- and Inter-molecular Electron Transfer Processes" (Grants I/77093 and I/79613 to J.H. and S.F.), and the Deutsche Forschungsgemeinschaft (Grant FE 383/7-1 to S.F.).

* To whom correspondence should be addressed. Prof. Dr. Susanne Fetzner, Institut für Molekulare Mikrobiologie und Biotechnologie, Westfälische Wilhelms-Universität Münster, Corrensstrasse 3, D-48149 Münster, Germany. Phone: +49 (0)251 83 39824. Fax: +49 (0)251 83 38388. E-mail: fetzner@uni-muenster.de.

‡ Universität des Saarlandes.

§ Westfälische Wilhelms-Universität Münster.

[1] Abbreviations: AOR, aldehyde oxidoreductase; bXOR, bovine xanthine oxidoreductase (from cow's milk); CO-DH, carbon monoxide dehydrogenase; DCPIP, 2,6-dichlorophenol indophenol; *Dd*AOR, aldehyde oxidoreductase from *Desulfovibrio desulfuricans*; *Dg*AOR, aldehyde oxidoreductase from *Desulfovibrio gigas*; EPR, electron paramagnetic resonance; FAD, flavin adenine dinucleotide; INT, iodonitrotetrazolium chloride; LB, lysogeny broth; MCD, molybdopterin cytosine dinucleotide; NAD^+, nicotinamide adenine dinucleotide, oxidized form; NBT, nitroblue tetrazolium chloride; *Oc*CO-DH, carbon monoxide dehydrogenase from *Oligotropha carboxidovorans*; PAGE, polyacrylamide gel electrophoresis; PCR, polymerase chain reaction; PMS, phenazine methosulfate; Qor, quinoline 2-oxidoreductase; *qorMSL*, genes coding for the three subunits of quinoline 2-oxidoreductase; Qox, quinaldine 4-oxidase; Qox_S, Qox_M, Qox_L, small, medium, and large subunit, respectively, of Qox; *qoxLMS*, genes encoding the three subunits of quinaldine 4-oxidase; *qoxL*, gene coding for the large subunit of quinaldine 4-oxidase; *qoxMS*, genes coding for the medium and small subunits of quinaldine 4-oxidase; rXOR, xanthine oxidoreductase from rat; *Rc*XDH, xanthine dehydrogenase from *Rhodobacter capsulatus*; SDS, sodium dodecyl sulfate; TB, terrific broth; Tris, tris(hydroxymethyl)-aminomethane; XO, xanthine oxidase; XOR, xanthine oxidoreductase.

10.1021/bi061185a CCC: $33.50
Published on Web 11/14/2006

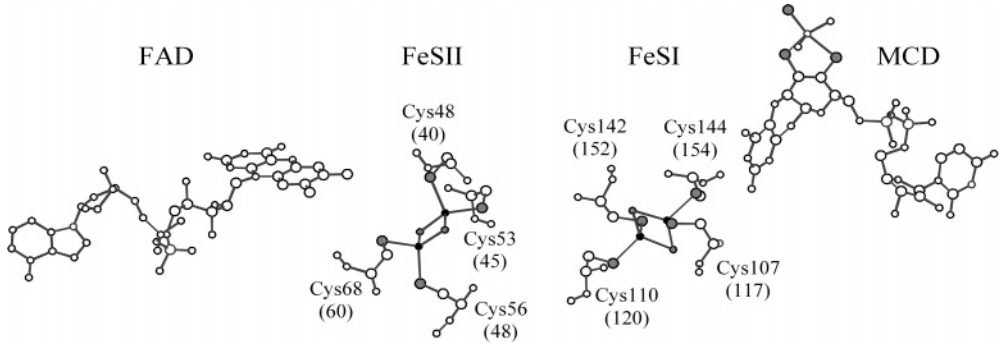

FIGURE 1: Topology of redox centers of quinoline 2-oxidoreductase (Qor) (*5*) as a model for Qox. The numbers in brackets refer to the corresponding amino acid positions in Qox. By convention, for FeSII the iron ion Fe1 is ligated by cysteines with the lower, Fe2 with the higher residue sequence numbers. Because of the unique fold of the FeSI-center, iron ion Fe1 is bound by the cysteine with the lowest sequence number and Fe2 by the cysteine next in sequence. MCD, molybdopterin cytosine dinucleotide; FAD, flavin adenine dinucleotide. Sulfur atoms are shown as gray, iron as black filled spheres.

structure and contains the molybdopterin cytosine dinucleotide form of the molybdenum cofactor (Mo−MCD), two distinct [2Fe-2S] clusters FeSI and FeSII, as well as FAD (*4*). A catalytically relevant glutamate residue, which in molybdenum hydroxylases of known structure is located close to the molybdenum center (*5*−*10*), seems to be conserved in Qox (E736 of the large subunit Qox_L). EPR redox titrations of Qox revealed widely separated midpoint potentials (versus standard hydrogen electrode) of −250 mV for FeSI and −70 mV for FeSII (*11*). The two iron-sulfur clusters and FAD are part of the electron-transfer pathway from the molybdenum center to the protein surface (*11*, *12*). This set of redox-active centers provides the enzyme with the capacity for holding a maximum of 12 electrons per native $(LMS)_2$ enzyme. Qox functions as an oxidase, generating H_2O_2 (*4*).

The two [2Fe-2S] centers of molybdenum hydroxylases can be distinguished by their different EPR properties (*g*-tensor principal values). By convention, the center with less anisotropic *g*-factors is named FeSI, the other FeSII. A general assignment of the FeSI and FeSII EPR signals to the FeS-cluster proximal and distal to the molybdenum cofactor, respectively, was derived from the analysis of dipolar interactions between these redox centers in bovine xanthine oxidoreductase (bXOR), isoquinoline 1-oxidoreductase of *Brevundimonas diminuta* 7, and aldehyde oxidoreductases (AOR) of *Desulfovibrio gigas* and *D. alaskensis* (*12*−*17*). Whereas the FeSII center resembles the plant-type [2Fe-2S] ferredoxins in its coordination motif, FeSI is characterized by a unique protein fold with an unusual amino acid motif and is found exclusively in enzymes of the xanthine oxidase family. Sequence-specific assignment of FeSI and FeSII to the C-terminal and N-terminal four-cysteine-motif, respectively, was established by mutagenesis of rat xanthine oxidoreductase (rXOR) (*18*). Comparative amino acid sequence analyses suggested that in Qox, FeSI is coordinated by the cysteine residues of motif $^{117}CGXCX_{31}CXC^{154}$ of the small subunit (Qox_S), whereas motif $^{40}CX_4CGXCX_{11}C^{60}$ of Qox_S binds FeSII (*19*). Fe1 of FeSI is thought to be linked to C117 and C154, and C120 and C152 should ligate the Fe2 ion. In the FeSII cluster, residues C40 and C45 are the presumed ligands of Fe1, while C48 and C60 should bind Fe2. This is illustrated in Figure 1, using the structure of quinoline 2-oxidoreductase (Qor) for comparison (*5*).

Recently, we have constructed *Pseudomonas putida* KT2440 pKP1, which synthesizes Qox in catalytically fully competent form (*19*). With this heterologous expression system, the *qoxLMS* genes are accessible to mutagenesis approaches. Substitution of a cysteine residue ligated to a [2Fe-2S]-cluster with serine replaces a sulfhydryl with a hydroxyl group, which should result in a serinate ligand to the iron, provided that the energetic difference between the generation of cysteinate and serinate is not a critical factor and the cluster is still assembled (*20*, *21*). Effects of individual cysteine-to-serine replacements on the cluster properties should be attributable to one of the two iron sites. In this study, site-directed mutagenesis was used to construct variants of Qox with replacements of positions C40, C45, C48, C60, C120, and C154 of Qox_S by serine, to assess which iron ions of FeSI and FeSII are likely to be involved in intramolecular electron transfer between the molybdenum center and flavin. Moreover, the conserved residue E736 of Qox_L was replaced by glutamine and aspartate to assess its potential role in catalysis.

EXPERIMENTAL PROCEDURES

Bacterial Strains and Plasmids. Bacterial strains and plasmids used are listed in Table 1. *P. putida* KT2440 (*22*, *23*) was used as a host for pKP1 (*19*) and its derivatives. In the pKP1 plasmids, transcription of *qoxLMS* genes, inserted into the expression vector pJB653 (*24*), is under the control of the *Pm* promotor and is activated by the XylS protein in the presence of (alkyl)benzoate. Plasmids pUC2.5 and pUCBamHI were constructed by subcloning a 2547 bp *Eco*RI-*Sma*I fragment and a 2248 bp *Bam*HI fragment of pKP1 into the *Eco*RI-*Sma*I sites and *Bam*HI site, respectively, of pUC18 (*25*). *Escherichia coli* DH5α (*26*) was used as a host for pUC2.5 and pUCBamHI and their derivatives.

Media and Growth Conditions. All *E. coli* strains were grown at 37 °C in lysogeny broth (LB) (*27*) containing 100 μg/mL ampicillin. For plasmid preparations, *P. putida* KT2440 harboring pKP1 or derivatives of pKP1 was grown at 29 °C in LB containing ampicillin. To generate biomass for protein purification, *P. putida* KT2440 pKP1 clones were grown in a 6 L bioreactor in mineral salt medium (*28*), supplemented with 1 g/L $(NH_4)_2SO_4$, and in the presence of ampicillin (500 μg/mL). Sodium benzoate (8 mM) was added repeatedly as a source of carbon and energy, and as XylS effector. As additional XylS effector, 2-methylbenzoate (2

Table 1: Bacterial Strains and Plasmids

bacterial strains and plasmids	description	source or reference
A. nitroguajacolicus Rü61a	wild-type strain utilizing quinaldine as sole source of carbon, nitrogen, and energy	(*1*)
E. coli DH5α	*endA1 hsdR17* (r_K^- m_K^+) *supE44 thi-1 recA1 gyrA96 relA1 deoR* Δ(*lacZYA-argF*)-*U169* ϕ80d*lacZ*ΔM15	(*26*)
P. putida KT2440	r^- derivative of *P. putida* mt-2	(*22*, *23*)
pUC18	ColE1 *lac*Z Ap^r	(*25*)
pKP1	*qoxLMS* (PCR amplificate) inserted in *Eco*RI and *Sma*I sites of pJB653	(*19*)
pUC2.5	2.5 kb *Eco*RI/*Sma*I fragment of pKP1 in *Eco*RI and *SmaI* sites of pUC18	this work
pUCBamHI	2.3 kb *Bam*HI fragment of pKP1 in *Bam*HI site of pUC18	this work
pKP1E736D, pKP1E736Q	pKP1 carrying mutation in *qoxL* for the production of Qox_LE736D and Qox_LE736Q, respectively	this work
pKP1C40S, pKP1C45S, pKP1C48S, pKP1C60S, pKP1C120S, pKP1C154S	pKP1 carrying a mutation in *qoxS* for the production of Qox_SC40S, Qox_SC45S, Qox_SC48S, Qox_SC60S, Qox_SC120S, and Qox_SC154, respectively	this work

Table 2: Primer Pairs Used for Site-Directed Mutagenesis of *qox* Genes

amino acid replacement	mutagenic primer pair[a]
QoxL: E736D	5′-TGCAGGAGA**C**ACGGCAACAGG-3′ 5′-GTTGCCGT**G**TCTCCTGCACCC-3′
QoxL: E736Q	5′-TTCCAAGG**G**TGCAGGA**C**AGACGGCAACAGG-3′ 5′-ACCTGTTGCCGTCT**G**TCCTGCACCCTTGG-3′
QoxS: C40S	5′-CGGGACCAAAGCCG**G**TT**C**CCTTGAAGC-3′ 5′-GCGCTTCAAGG**G**AACCG**G**CTTTGG-3′
QoxS: C45S	5′-TGAAGCGCGGT**C**TGGCAGTTGCAGC-3′ 5′-GCAACTGCCA**G**ACCGCGCTTCAAGG-3′
QoxS: C48S	5′-TGTGGCAGTT**C**CAGCGTCCATGTC-3′ 5′-ACATGGACGCTG**G**AACTGCCACACC-3′
QoxS: C60S	5′-ATCAAGGCCT**C**CAACGTACTAGC-3′ 5′-TGATACGTTG**G**AGGCCTTGATGAGC-3′
QoxS: C120S	5′-TGTGGCTACT**C**CACGCCGGGTATGC-3′ 5′-ACCCGGCGTG**G**AGTAGCCACACTGC-3′
QoxS: C154S	5′-CTGTGCAGGT**C**CACCGGCTATCAGACC-3′ 5′-GATAGCCGGTG**G**ACCTGCACAGATTGC-3′

[a] Bold and underlined letters indicate the mutagenic nucleotides.

mM) was added at an optical density (600 nm) of 0.8−1.2. At an optical density (600 nm) of about 4, cells were harvested by centrifugation at 14000*g* for 15 min at 4 °C. For the preparation of electrocompetent cells, *E. coli* DH5α and *P. putida* K T2440 were cultured in TB (*27*).

Recombinant DNA Techniques. DNA restriction, dephosphorylation and ligation reactions, and agarose gel electrophoresis was performed by standard procedures (*27*). Plasmid DNA was prepared using the E.Z.N.A. Plasmid Miniprep kit I (PeqLab, Erlangen, Germany). DNA fragments were purified from gel slices using the Nucleo Spin Extraction kit of Macherey-Nagel (Düren, Germany). *E. coli* DH5α and *P. putida* KT2440 host cells were transformed by electroporation.

Site-Directed Mutagenesis. Site-directed mutagenesis of *qox* genes was performed according to the protocol of the QuikChange site-directed mutagenesis kit (Stratagene, Heidelberg, Germany) using pUC2.5 and pUCBamHI as templates, and *Pfu* polymerase for amplification. The mutagenic primer pairs are listed in Table 2. All pUC2.5 and pUCBamHI derivatives were subcloned in *E. coli* DH5α, and each mutation was verified by DNA sequencing (MWG Biotech, Ebersberg, Germany). The *Eco*RI-*Sma*I and the *Bam*HI fragments carrying the respective mutations were gel purified and ligated into pKP1Δ(*Eco*RI-*Sma*I-fragment) and pKP1Δ-(*Bam*HI-fragment), respectively. In each case, correct insertion of the fragment was verified by restriction and sequence analysis.

Purification of Qox and Qox Variants and Enzyme Assays. Preparation of cell extracts and protein purification were performed as described previously (*19*). The activity of Qox proteins was measured spectrophotometrically by following the quinaldine-dependent reduction of the artificial electron acceptor INT (iodonitrotetrazolium chloride) ($\epsilon_{503\ nm} = 19.3$ mM^{-1} cm^{-1}; *29*). Determinations of apparent K_m and k_{cat} values of electrophoretically pure Qox proteins were carried out in triplicate. To determine the apparent kinetic constants of the enzyme for one substrate, saturating concentrations of the other substrate were used. Apparent K_m values were deduced from Hanes plots. The activity of Qox and Qox variants with dioxygen as electron acceptor was determined in air-saturated buffer by measuring formation of 1*H*-4-oxoquinaldine at 325 nm ($\epsilon_{325\ nm} = 8.4$ mM^{-1} cm^{-1}; *4*). Enzyme activity with other electron acceptors was investigated under anoxic conditions. The assay mixture, containing 77 mM Tris/HCl, pH 8.5, 5.6 mM quinaldine, and electron acceptor solution, was placed in an anaerobic cuvette and gently bubbled with oxygen-free nitrogen for more than 10 min. The enzyme solution (0.14−2.8 U/mg) in the sidearm was treated in the same way, and the reaction was started in the closed cuvette by addition of the enzyme solution out of the sidearm into the main compartment. Saturating concentrations of each oxidizing substrate were as follows: 187 μM of ferricyanide, 1,4-benzoquinone, 1,2-naphthoquinone, or methylene blue; 93 μM of DCPIP; 1.87 mM of INT; 467 μM (93.4 μM for Qox_SC40S and Qox_SC60S) of PMS; 93 μM (46.5 μM for Qox_SC40S) of thionine; 93 μM of NBT; 187 μM (561 μM for Qox) of Meldola blue. Reduction of electron acceptors was measured photometrically in the case of $K_3[Fe(CN)_6]$ ($\epsilon_{420\ nm} = 1.02$ mM^{-1} cm^{-1}; *30*), DCPIP

($\epsilon_{600\ nm}$ = 21.0 mM^{-1} cm^{-1}; *31*), PMS ($\epsilon_{388\ nm}$ = 22 mM^{-1} cm^{-1}; *32*), NBT ($\epsilon_{566\ nm}$ = 28.6 mM^{-1} cm^{-1}; *33*), and Meldola blue ($\epsilon_{569\ nm}$ = 13.9 mM^{-1} cm^{-1}; *34*). In the assays with 1,4-benzoquinone, 1,2-naphthoquinone, thionine, methylene blue, indigotetrasulfonate, indigotrisulfonate, indigocarmine, alloxazine, anthraquinone, NAD^+ and methylviologen as potential electron acceptors, formation of 1*H*-4-oxoquinaldine was monitored at 325 nm. Specific activity of Qox proteins was defined as micromoles of product formed, or micromoles of electron acceptor reduced, per minute and per milligram of protein. In the case of the one-electron acceptor $K_3[Fe(CN_6)]$, Qox specific activity was defined as two micromoles of $K_3[Fe(CN_6)]$ reduced per minute and per milligram of protein. Protein concentrations were estimated by the method of Lowry et al. (*35*) using bovine serum albumin as standard protein.

Reductive Titration of Qox Proteins with Sodium Dithionite. Reduction of Qox proteins by dithionite were carried out under anoxic conditions. Solutions of enzyme and reductant (in 100 mM Tris/HCl, pH 8.5) were gently bubbled with oxygen-free nitrogen for more than 10 min and incubated for 30 min in an anaerobic glove box in an atmosphere of 95% N_2, 5% H_2. In the glove box, the enzyme solution was put in an anaerobic cuvette and overlaid with argon; a gastight syringe was filled with dithionite solution and inserted into the septum of the anaerobic cuvette. Aliquots of dithionite solution were injected, and UV/vis absorption spectra were recorded with a Jasco V-550 UV/vis spectrophotometer after each addition of dithionite. For calibration, a solution of FAD of known concentration was titrated with sodium dithionite.

Anaerobic Reduction of Qox Proteins with Quinaldine. In the anaerobic glove box, protein solution (in 100 mM Tris/HCl, pH 8.5) was filled into the main compartment of an anaerobic cuvette, and a 20-fold molar excess of quinaldine dissolved in isopropanol was put in the side arm. The reaction was started by mixing the two solutions, and absorbance spectra were recorded repeatedly.

Polyacrylamide Gel Electrophoresis (PAGE). Nondenaturing PAGE was carried out in 8% T, 2.6% C resolving gels using the system described by Laemmli (*36*) but omitting SDS from the gels. Proteins were stained with Coomassie blue R-250 (0.1% [w/v] in 50% [w/v] trichloroacetic acid). For activity staining of Qox proteins, nondenaturing PA gels were immersed in the same assay mixture as used for the spectrophotometric assay; gel slices incubated in buffer and INT, without quinaldine, were used as controls.

EPR Spectroscopy. EPR spectra were recorded at X-band frequencies (9.5 GHz) on Bruker ESP300 and Bruker ESP300E spectrometers equipped with an Oxford ESR 900 liquid helium flow cryostat. In all cases, samples were frozen in liquid nitrogen in 4-mm quartz EPR tubes (Wilmad). Because of the limited amounts of sample material, the experiments were performed in consecutive steps. First, the sample "as isolated" was measured to monitor the presence of "background" signals or of known inactive forms such as the resting Mo(V)-species, usually present in preparations in small amounts. Then, under anaerobic conditions, the samples were reacted with the substrate quinaldine in a 20-fold molar excess inside the EPR tube. If no signals were detected the molar excess was increased to 60-fold or even 100-fold. In a third step, these samples were reduced completely by a 20-fold molar excess of dithionite and measured at temperatures between 10 and 80 K. The magnetic field and the microwave frequency were determined with a NMR gaussmeter and a microwave counter, respectively. The modulation amplitude for spectra recording generally was 0.5 millitesla (mT). For measurements below 80 K, spectra were recorded at variable microwave powers (2.0−20.0 mW) to avoid saturation broadening. The conversion time and time constant were 50 ms. Because the lowest absolute amount of enzyme in the sample was only 3.5 nmol (i.e., 7 nmol of each type of center), spectra had to be accumulated up to 150 times under optimized EPR settings and baseline corrected.

To obtain a quantitative estimate of the relative iron content within the [2Fe-2S] centers, the corrected spectra of the dithionite reduced protein variants, recorded under standardized EPR conditions (2 mW microwave power, 20 K), were doubly integrated (XeprView and WinEPR, Bruker BioSpin). The resulting values were then compared to that of recombinant Qox, which was prepared in the same way as the variant proteins, and normalized for the amount of protein in each sample, and, if necessary, for different width of field sweep and number of spectra additions. The error of the integration procedure was found to be 10−25% depending on the signal-to-noise ratio and the quality of the background subtraction.

The relative proportion of the two [2Fe-2S] centers was estimated by reconstruction of the experimental spectra of the dithionite reduced samples. For that purpose, each cluster of the various proteins was simulated separately, and the resulting spectra were normalized to give the same double integral value. The experimental pattern was then reconstructed by a weighted addition of the normalized simulated spectra focusing on a close fit of the g_1- and the resolved g_3-components. The sum of the relative contributions was normalized to one, so that a ratio for I/II of 0.5/0.5 indicates an equal population of both cluster sites. A shift in the ratio to, say, 0.4/0.6 then means that the population (or occupation) of the FeSI component is only 40% and that a maximal fraction of 2·0.4 = 0.8 (80%) of the protein portion loaded with FeS-iron (i.e., the relative iron content) can have both FeS-sites occupied. Therefore, multiplying this value with the relative iron content yields an estimate of fully active molecules, which is finally used to normalize the $k_{cat\ app}$ values. With this procedure, two essential effects of the amino acid substitution in Qox proteins, the loss of iron and an unbalanced population of the FeS-centers, are taken into account for the determination of the kinetic constants. In this simplified model, the difference between the values of ratio I/II, e.g., a fraction of 0.2 in the above example, then represents singly occupied FeS-sites. The approach implicitly assumes that for the FeS-center with the lower value in the ratio I/II, the site of the other FeS-center is always occupied, and thus gives an estimate of the maximum population of fully occupied enzyme molecules. In cases for which the spectral contribution of FeS-centers I and II could not be clearly separated or unassignable lines appeared, the relative iron content alone was used to obtain an upper estimate of the normalized $k_{cat\ app}$ value. Because some of the experimental spectra are governed by strong *g*-strain effects, the simulations were not perfect in such cases. The error margins were estimated from the differences of possible multiplication

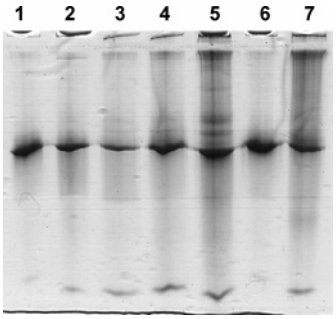

FIGURE 2: Nondenaturing polyacrylamide gel of purified Qox proteins, stained with Coomassie Blue. Lane 1: recombinant Qox from *P. putida* KT2440 pKP1; 2: Qox_LE736D; 3: Qox_LE736Q; 4: Qox_SC40S; 5: Qox_SC48S; 6: Qox_SC60S; 7: Qox_SC120S.

factors in the range of ± 0.05 and ± 0.1 depending on the quality of the fit to experimental patterns.

RESULTS AND DISCUSSION

Purification of Recombinant Qox and Qox Variants. Recombinant Qox and Qox variants were isolated from the soluble fraction of cell extracts of the respective *P. putida* KT2440 pKP1 clones. The system for heterologous expression of the *qoxLMS* genes does not result in overexpression, and the yield of the four-step purification procedure is only approximately 5−10% (*19*), so the limited availability of protein constrained quantitative studies. In nondenaturing PAGE (Figure 2) and in gel filtration, the mobility of the protein variants corresponded to that of recombinant Qox, indicating that each protein was correctly assembled to form the $(LMS)_2$ multimer. In case of Qox_SC45S[2] and Qox_SC154S, which could not be obtained as pure proteins using the established protocol, activity staining of the protein preparations separated in nondenaturing PAGE confirmed that they migrate like wild-type Qox (data not shown). Enrichment of the Qox_SC154S protein by hydrophobic interaction chromatography and gel filtration resulted in an about 1.3- and 2.5-fold reduction of specific activity, respectively, despite removal of contaminating proteins as evident from PAGE. The Qox_SC45S protein also was less stable than Qox, as indicated by a decrease in activity with time. These observations suggest conformational instability of Qox_S-C154S and Qox_SC45S, or a loss of redox centers, or both. Despite some changes in the UV/vis absorption features of Qox proteins carrying cysteine-to-serine substitutions, the optical spectra of the purified Qox variants were still characteristic for molybdo-iron/sulfur flavoproteins (Figure 3).

EPR and UV/vis-Spectral Properties of Recombinant Qox. In a preceding study (*19*), the recombinant Qox protein produced by the expression clone *P. putida* KT2440 pKP1 was characterized biochemically and spectroscopically and compared to Qox from the wild-type strain *A. nitroguajacolicus* Rü61a. The results demonstrated the presence and integrity of the redox centers in recombinant Qox, and similar kinetic properties of wild-type and recombinant Qox. In the EPR spectra, only minor differences for the axial FeSI signal, unique for all Qox species, have been observed, indicating highly similar or identical redox behavior and local environments of the centers. When recombinant Qox, prepared in the same way as the variant enzymes, was reduced under anoxic conditions with a 20-fold molar excess of its substrate quinaldine, a reduction level of 91% of the initial absorbance at 450 nm was reached immediately after substrate addition. A second, much slower phase of reduction took about 90 min to reach the endpoint (Figure 3A). Such biphasic reaction was already observed by Leimkühler et al. (*6*) for reduction of *Rc*XDH by xanthine. The authors suggested that the fast phase constitutes the population of fully active enzyme molecules, whereas the population of protein that is reduced in the second, much slower phase consists of catalytically inactive enzyme which is reduced by intermolecular electron transfer from the reduced functional proteins. On the basis of this hypothesis, the kinetics of reduction of Qox by quinaldine suggests that more than 90% of the enzyme is fully active.

The corresponding EPR spectra of the recombinant Qox protein are shown in Figure 4a. In the presence of the organic substrate quinaldine, the Mo(V) very rapid species and a weak signal of FAD semiquinone can be observed together with the characteristic signal of FeSII and a small amount of FeSI at low temperatures (spectra A and B). After reduction with dithionite the FAD signal and the very rapid species are hardly visible, but both [2Fe-2S] cluster signals are present (spectrum C). Their spectral reconstruction yields a ratio I/II (Table 4) characteristic for an equal population of the FeS-center sites within error limits. The temperature dependence shown in Figure 4b is identical to that found for Qox from the wild-type strain *A. nitroguajacolicus* Rü61a, with the FeSII signal typically vanishing above 35 K. It can be inferred from the EPR spectra obtained after reduction with substrate that electrons are mainly residing on the catalytic intermediary Mo(V)-species and the FeSII center, and to a smaller extent at FAD and FeSI. The degree of FeSII reduction in the presence of substrate is about 0.7 as derived from a comparison of signal intensity of the dithionite reduced sample. As with xanthine oxidase, electron distribution on the redox-active centers in Qox is assumed to be directed by the relative redox potential of the centers (*37*).

The anoxic reductive titration of recombinant Qox (15 nmol, corresponding to 30 nmol of each redox center) with sodium dithionite was followed by UV/vis spectroscopy at 450 and 550 nm and compared to the reduction behavior of an FAD solution (30 nmol in the same buffer as the protein, anoxic conditions) (Figure 5). For the solution of free FAD, the A_{450} value was lowered to 50% with respect to the endpoint of titration upon addition of 75 nmol of dithionite, which corresponds to 1 mol of reducing equivalent per mol FAD. In contrast, for Qox half of the maximal ΔA_{450} value (difference of extinction in non-reduced and fully reduced state) was already reached after addition of 45 nmol dithionite, whereas the ΔA_{550} dropped to 50% for 75 nmol dithionite added. At this stage, the ΔA_{450} value was reduced to about 20% of initial absorbance. Because Qox was previously shown to generate the anionic (red) semiquinone species upon reduction (*11*), the absorption at 550 nm is mainly due to the FeS-centers. This allows one to estimate

[2] The subscript L or S after Qox indicates that the numbering of the following residue refers to the sequence of the small and large subunit, respectively.

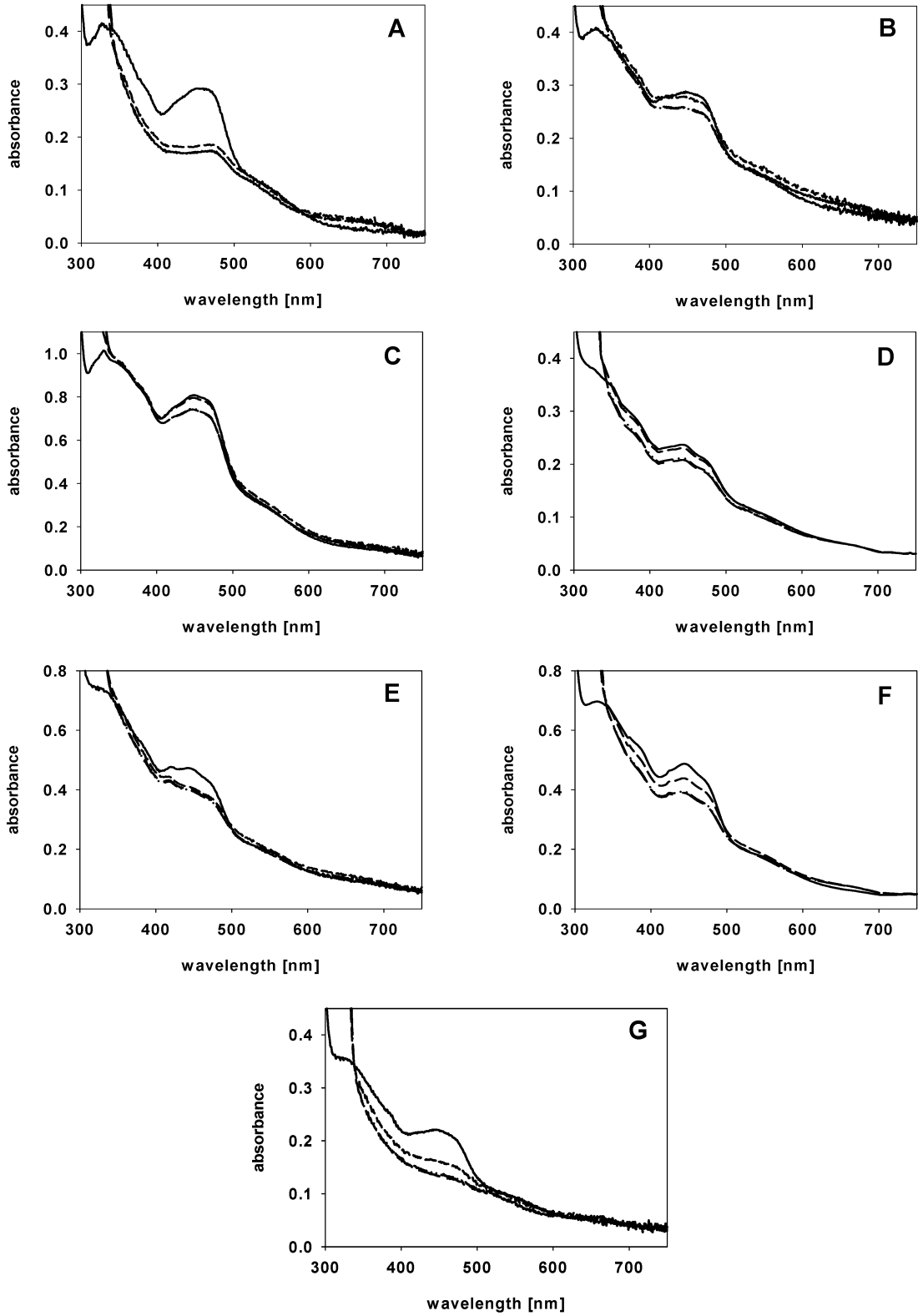

FIGURE 3: UV/vis absorption spectra of Qox and Qox variants upon reduction with quinaldine under anoxic conditions. (A) recombinant Qox (16.1 μM); (B) Qox_LE736D (10.5 μM); (C) Qox_LE736Q (23.7 μM); (D) Qox_SC40S (14.2 μM); (E) Qox_SC48S (22 μM); (F) Qox_S-C60S (8.6 μM); (G) Qox_SC120S (9.8 μM) in 100 mM Tris/HCl, pH 8.5. Proteins as isolated (−) and after 15 s (---), 90 min (− • • −), and 110 min (− − −) of incubation with a 20-fold molar excess of quinaldine.

the values of FAD reduction at 450 nm assuming that about 50% of the total absorption at this wavelength is caused by FAD or FeS-centers, respectively. From that it is estimated that the FAD in Qox is half reduced at 40 nmol of dithionite added. After addition of 75 nmol of dithionite, when the FeS-centers are reduced by about 50%, only 5% of FAD is left in the oxidized state. These findings indicate that the redox potential of FAD in Qox is clearly more positive than that of the free FAD (−200 to −300 mV). They qualitatively also agree with the redox potentials of the [2Fe-2S] centers in Qox (FeSII : −70 mV, FeSI: −250 mV) (*11*). With 75 nmol of dithionite added, the FeSII centers should be nearly

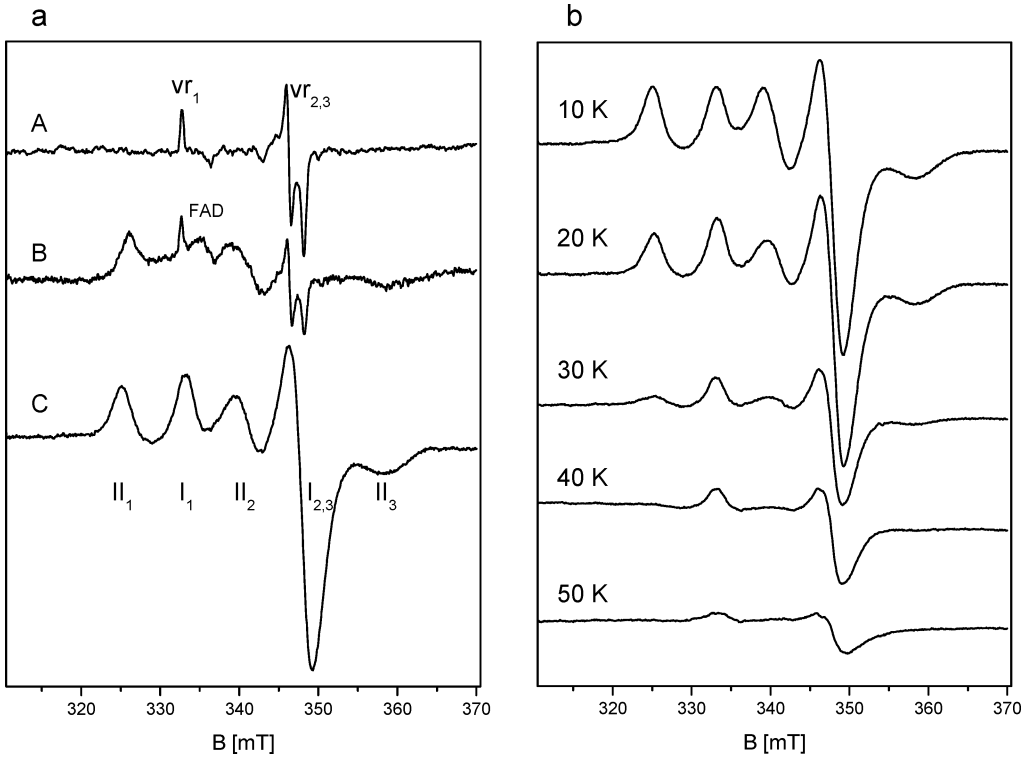

FIGURE 4: EPR spectra of recombinant Qox from *P. putida* KT2440 pKP1 reduced under anoxic conditions. Panel a shows the spectra obtained after reduction with an excess of quinaldine at 80 K (trace A) and 20 K (trace B), and with dithionite at 20 K (trace C). Panel b illustrates the temperature behavior of the [2Fe-2S] centers after dithionite reduction. The assignment of redox-active centers is indicated (vr: very rapid species; FAD: FAD semiquinone radical; II and I: iron sulfur centers I and II, indices indicate the *g*-tensor components).

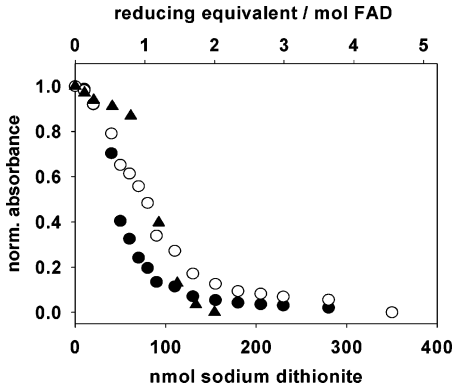

FIGURE 5: Reductive titration of FAD (30 nmol; triangles) and recombinant Qox (15 nmol; circles) with sodium dithionite under anoxic conditions. The points are measured absorbance values from spectra taken after each addition of dithionite; filled and open symbols indicate normalized (norm) absorbance at 450 and 550 nm, respectively. The number of reducing equivalents was calculated from the amount of added dithionite. Two reducing equivalents were defined as the amount of dithionite required for the full reduction of 1 FAD to $FADH_2$.

completely reduced, so that the residual absorption should mainly arise from FeSI-centers.

Properties of Qox Variants Substituted at E736 of QoxL. All enzymes of the XO family studied to date contain a strictly conserved glutamate residue, which in the structures of *Rc*XDH, bXOR, *Oc*CO-DH, *Dg*AOR, *Dd*AOR, and Qor is located at about 3−4 Å from the molybdenum (*5*−*10*, *38*). On the basis of the crystal structure of bXOR with a slow substrate, Okamoto et al. (*39*) recently proposed that this conserved glutamate initiates catalysis by acting as a general base that abstracts a proton from [Mo(VI)-OH]. Comparison of amino acid sequences suggested that E736 is the corresponding conserved glutamate residue of Qox. If this residue acts as the catalytic base of Qox, its replacement should drastically affect the substrate turnover rate. The catalytic activity of the Qox_LE736Q protein indeed was below the detection limit of the spectrophotometric standard assay. After incubation of Qox_LE736Q with quinaldine for up to 14 h under oxic conditions (i.e., with O_2 as electron acceptor), formation of the organic product 1*H*-4-oxoquinaldine was not detectable spectrophotometrically. However, prolonged activity staining of protein preparations separated in nondenaturing polyacrylamide gels revealed a red band due to formation of $INTH_2$, indicating that quinaldine-dependent reduction of the protein and electron transfer to its artificial electron acceptor still occurred. Remarkably, replacement of E736 by aspartate, which retains the functional group (but should result in an altered distance between carboxylate group and molybdenum center), yielded a Qox protein with a lower but still significant residual activity of 0.016 U/mg (standard assay) and an apparent K_m value for quinaldine quite similar to that of Qox (Table 3).

The optical absorption spectra of the Qox_LE736D and Qox_LE736Q proteins (as isolated) resemble that of Qox (Figure 3, Table 4). Anoxic reduction by quinaldine was slow and reached the endpoint after 90 (Qox_LE736D) and 110 min (Qox_LE736Q); in both proteins, the extent of reduction by quinaldine was significantly lower than observed for Qox (Figure 3B,C). This UV/vis spectroscopic evidence of an impeded reduction by quinaldine is supported by EPR observations for the quinaldine-reduced enzyme. Different from Qox, no very rapid Mo(V) species could be detected in Qox_LE736Q or Qox_LE736D after reduction with substrate, but a weak signal, presumably of FAD semiquinone, was present at 80 K. At lower temperatures mainly the FeSII

Table 3: Apparent Kinetic Constants of Purified Qox Proteins[a]

Qox protein	$K_{m\ app}$ (quinaldine) [M]	$k_{cat\ app}$ (quinaldine) [s^{-1}]	normalized[b] $k_{cat\ app}$ (quinaldine) [s^{-1}]	$K_{m\ app}$ (INT) [M]	$k_{cat\ app}$ (INT) [s^{-1}]	normalized[b] $k_{cat\ app}$ (INT) [s^{-1}]
Qox from *P. putida* KT2440 pKP1	3.8×10^{-5} ($\pm 0.2 \times 10^{-5}$)	19.3 ($\pm$0.7)	19.3	7.6×10^{-5} ($\pm 1.7 \times 10^{-5}$)	12.7 ($\pm$0.7)	12.7
Qox_LE736D	2.7×10^{-5} ($\pm 0.4 \times 10^{-5}$)	0.11 ($\pm$0.004)	0.4	5.0×10^{-5} ($\pm 0.9 \times 10^{-5}$)	0.5 ($\pm$0.04)	5.1
Qox_SC40S	3.8×10^{-5} ($\pm 0.2 \times 10^{-5}$)	1.1 ($\pm$0.01)	2.7	4.3×10^{-5} ($\pm 0.8 \times 10^{-5}$)	0.6 ($\pm$0.03)	1.5
Qox_SC48S	5.2×10^{-5} ($\pm 0.7 \times 10^{-5}$)	10.6 ($\pm$0.4)	17.7	5.4×10^{-5} ($\pm 0.5 \times 10^{-5}$)	7.2 ($\pm$0.06)	12
Qox_SC60S	2.9×10^{-5} ($\pm 0.9 \times 10^{-5}$)	3.2 ($\pm$0.3)	10.0	4.2×10^{-5} ($\pm 0.9 \times 10^{-5}$)	3.1 ($\pm$0.2)	9.7
Qox_SC120S	3.1×10^{-5} ($\pm 0.2 \times 10^{-5}$)	2.9 ($\pm$0.05)	9.5	3.4×10^{-5} ($\pm 0.3 \times 10^{-5}$)	2.2 ($\pm$0.04)	7.5

[a] Because of negligible activity and/or instability, it was not possible to determine the kinetic constants of Qox_LE736Q, Qox_SC45S, and Qox_SC154S. [b] Assuming that the relative iron content of a protein preparation together with the fraction of molecules with both FeS-cluster sites occupied (Table 4) reflects the population of fully active molecules, k_{cat} values were normalized to the corresponding fraction of protein. For Qox and Qox_SC40S, however, the relative iron contents of 1 and 0.41, respectively, were used for normalization of $k_{cat\ app}$.

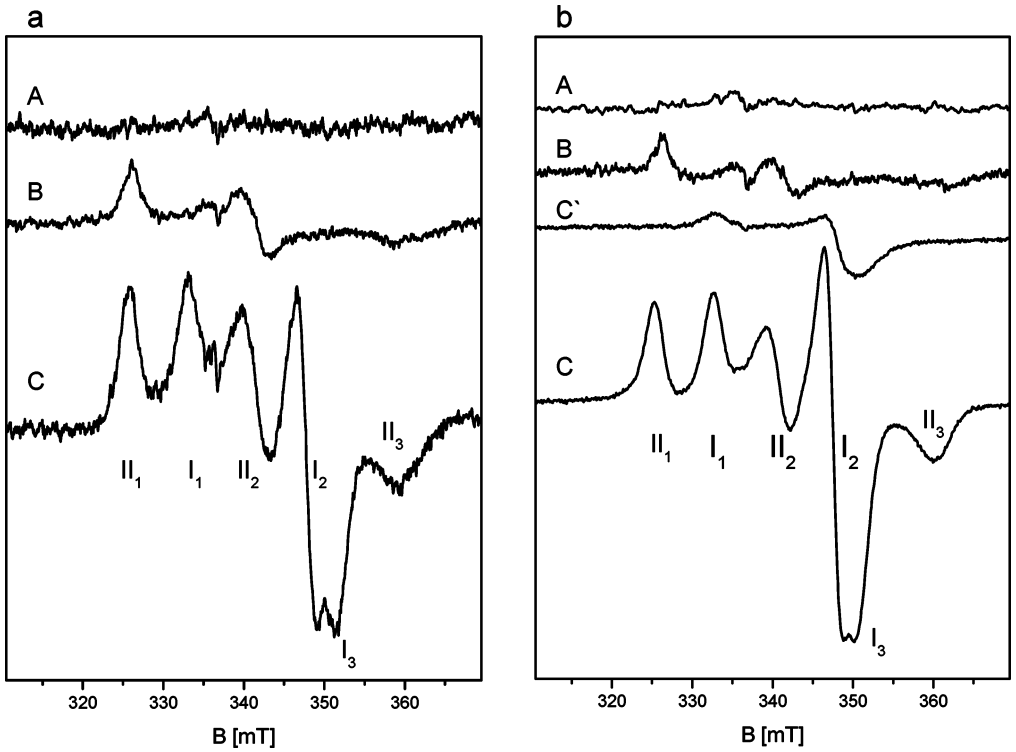

FIGURE 6: EPR spectra of Qox_LE736D (panel a) and Qox_LE736Q (panel b) reduced anaerobically with quinaldine (spectra A and B in both panels) and fully reduced with dithionite (C and C′). The spectra A were recorded at 80 K, spectrum C′ was recorded at 50 K, and the other ones were obtained at 20 K.

signal pattern was observed. Subsequent reduction with dithionite produced the typical [2Fe-2S] cluster patterns for which resolved rhombic distortions of the axial component of FeSI become apparent (Figure 6 a,b, compare to Figure 4 signal $I_{2,3}$, Table 4). The corresponding ratios of FeSII signal intensity were 0.25 for Qox_LE736D and 0.075 for Qox_LE736Q, again indicating a rather restrained reduction of the proteins by quinaldine. The absence of any Mo(V)-species (very rapid, rapid) in Qox_LE736D and Qox_LE736Q requires that the Mo-MCD cofactor is either fully oxidized or reduced (Mo(VI) or Mo(IV)), both states being EPR silent. The protein variants show a significantly smaller activity as inferred from the ratios of the FeSII signals upon quinaldine addition in comparison to Qox, but they are still active. This implies that the catalytic Mo(V) intermediate (very rapid signal) is formed in much lower amounts and is less stable than in the wild type, so that no EPR intensity is built up under the conditions applied.

For both enzyme variants, fully reduced with dithionite, double integration of the EPR spectra was used to estimate the relative iron content with respect to recombinant Qox yielding about 34% for Qox_LE736D and 50% for Qox_LE736Q (Table 4). These values are indicative for a destabilization of the iron clusters during holoenzyme assembly and/or protein preparation, producing considerable loss of iron in both variants. From a reconstruction of the individual FeS-center contributions (see Experimental Procedures), a small but significant lowering of the FeSI portion vs FeSII is observed (ratio I/II in Table 4) in comparison to recombinant Qox, indicating that the remote substitution at E736 affects the occupation of the FeSI site slightly stronger than the FeSII site. This implies that only a fraction of protein molecules can have the complete set of FeS-centers. In case of Qox_LE736D, this fraction corresponds to twice the occupation value for FeSI, i.e., 0.86. This value together with the relative iron content of 0.34 (Table 4) is used to normalize

Table 4: Relative Iron Content, EPR Parameters of the [2Fe-2S] Centers, and UV/vis Absorbance Ratios of Qox and Qox Variants

Qox protein	relative iron content	ratio of reconstructed FeS signals I/II (error margin)	FeSI			FeSII			A_{280nm}/A_{450nm}	A_{450nm}/A_{550nm}
			g_1	g_2	g_3	g_1	g_2	g_3		
Qox (recombinant)	1	0.53/0.47 (±0.05)	2.021	1.937	1.937	2.072	1.975	1.877	5.1	3
Qox_LE736D	0.34	0.43/0.57 (±0.05)	2.021	1.936	1.916	2.067	1.971	1.874	5.3	3.1
Qox_LE736Q	0.50	0.44/0.56 (±0.05)	2.024	1.937	1.923	2.070	1.976	1.869	5.4	3.2
Qox_SC40S	0.41	[1/0][c]	2.021	1.939	1.923				6.2	2.5
Qox_SC45S[a]	(0.05−0.09)[a]	n.d.[d]	2.010	1.935	1.935	2.038	1.910	1.895[b]	n.d.	n.d.
Qox_SC48S	1	[0.3/0.7][c] (±0.1)	2.021	1.934	1.934	2.028	1.934	1.881[b]	7.8	3.4
Qox_SC60S	0.38	0.58/0.42 (±0.1)	2.018	1.935	1.927	2.072	1.967	1.831	7.0	3.1
Qox_SC120S	0.47	0.69/0.31 (±0.1)	2.006	1.938	1.915	2.071	1.975	1.881	8.3	2.5
Qox_SC154S[a]	(0.10−0.30)[a]	0.83/0.17(±0.1)	2.009	1.909	1.760	2.066	1.977	1.875	n.d.	2.5

[a] Preparations contain contaminating proteins. [b] Tentative assignment, see text. [c] A clear identification of the individual cluster in the EPR spectra was not feasible, see text. [d] n.d., not determined.

the apparent k_{cat} value, yielding 0.38 s^{-1}, which is considerably smaller than the value determined for the recombinant protein (Table 3). It is evident from the marked decrease in $k_{cat\ app}$ for quinaldine (Table 3) that the replacement affected turnover of the heterocyclic substrate. The catalytic properties of Qox_LE736D generally resembled those of the corresponding variant of Qor, Qor_LE743D (*5*). In contrast, protein variants of *Rc*XDH carrying E730A, E730Q, E730R, and E730D replacements were inactive (*6*).

The observation of some reduction of the redox centers of the Qox_LE736Q protein by quinaldine suggests that either nucleophilic attack on quinaldine by the catalytic [Mo(VI)-OH] and concomitant hydride transfer from substrate to [Mo(VI)═S] to form [Mo(IV)-SH] very slowly occur even in the absence of glutamate-catalyzed proton abstraction from the [Mo(VI)-OH] group, or residues other than E736 can activate the hydroxy group to some extent. Since formation of the organic product 1*H*-4-oxoquinaldine by Qox_LE736Q was not detected, we may suggest that a Mo(IV)-O-quinaldine intermediate is formed but remains coordinated to the molybdenum center.

It is noted that the change of the side chain length and of the side chain polarity introduced by the substitution of E736 by aspartate and glutamine close to the molybdenum center also affects the stereochemical environment of the FeSI center. This is manifested by an increase of the rhombicity of the signals I_2, I_3 observed for Qox_LE736Q and more pronounced for Qox_LE736D compared to recombinant Qox (Figure 6a and b, spectra C). The alteration is transmitted over a distance of presumably 14−15 Å (using the structure of Qor for comparison), probably via modulation of the backbone and H-bonds in the vicinity of the Mo- and FeSI-center. In the case of Qox_LE736D, the shorter side chain might additionally affect the relative arrangement of the FeSI-center and the molybdenum pyranopterin cofactor, which may directly contact a cysteine ligand of FeSI via its amino substituent (as inferred from the structures of *Oc*CO-DH, *Dg*AOR, *Dd*AOR; bXOR, and *Rc*XDH (*8*−*10*, *40*−*42*). Such changes can modify the electron-transfer rates and the local redox potentials (which have not been determined yet).

Qox Variants Carrying Cysteine to Serine Replacements. Cysteine residues proposed to be ligands to the iron ions of FeSI and FeSII of Qox were individually replaced by serine to examine the effect on the properties of the cluster by UV/vis and EPR spectroscopy. Residues C154 and C120, as presumed ligands of Fe1 and Fe2, respectively, were chosen for the substitution at FeSI. In case of FeSII, each of the four cysteine ligands of FeSII was individually replaced by serine, since two of the replacements at FeSII (C45 and C40) appeared to disturb the integrity of the FeS center(s). Substitution of cysteine ligands in [2Fe-2S] ferredoxins by serine was reported to conserve the cluster in many cases, but the replacement may change the optical spectra as well as the EPR-signatures of the proteins, and affect their redox properties (*18*, *20*, *21*, *43*−*45*). It was found that all Qox variants, except Qox_SC48S, showed a significantly lower iron content, a variable occupation of the FeS-centers and partially drastic spectral changes compared to Qox. Therefore, the spectra integration and reconstruction (see Experimental Procedures) was also applied to analyze the kinetic properties of the Qox variants with cysteine to serine substitutions. The relevant values for an estimate of the apparent kinetic constants (Table 3) are listed in Table 4.

UV/vis Spectra and Catalytic Activities. The absorption spectra of the purified Qox variants carrying cysteine-to-serine replacements clearly showed some differences compared to the UV/vis spectrum of Qox (Figure 3, Table 4). Spectra of Qox_SC40S, Qox_SC48S, Qox_SC60S, and Qox_S-C120S were characterized by higher $A_{280\ nm}/A_{450\ nm}$ absorbance ratios, which probably indicate a lower content of chromophores. However, bandshifts in the 450 nm region due to replacement of a sulfur by an oxygen ligand may contribute to the observed spectral changes. Hypsochromic shifts of about 20 nm in the 400−500 nm region, as compared to the spectrum of wild-type protein, have been reported previously for [2Fe-2S] ferredoxins with noncysteinyl ligands (*43*, *44*). For native molybdenum hydroxylases, a ratio A_{450nm}/A_{550nm} of about 3 was proposed to indicate stoichiometric amounts of FAD:Fe:S of 1:4:4 (*46*). For bXOR, the absorbance in the 450 nm region is approximately 50% due to flavin, and 50% due to FeS, whereas absorbance at wavelengths > 530 nm is due only to FeS (*47*). Most of the Qox proteins carrying replacements of cysteine ligands by serine showed modified A_{450nm}/A_{550nm} ratios (Table 4), which may well reflect some loss of cofactor, or differences in ligand coordination to the respective FeS cluster, or both.

All the Qox variants that were amenable to purification and analysis showed apparent K_m values for quinaldine and INT similar to those of recombinant Qox, suggesting that the replacements did not significantly affect binding of these substrates (Table 3). The specific activities of recombinant Qox and the variants C40S, C48S, C60S, and C120S with a

Table 5: Specific Activities of Qox and Qox Variants (as Isolated) with Oxidizing Substrates

		specific activity (U mg^{-1})				
electron acceptor	standard redox potential E'_0 (mV)	Qox (rec.)	Qox_SC40S	Qox_SC48S	Qox_SC60S	Qox_SC120S
$K_3[Fe(CN)_6]$	+360[a]	1.03	0.045	0.50	0.11	0.38
O_2	+295[b]	3.14	0.060	1.16	0.45	1.14
1,4-benzoquinone	+286[c]	1.72	0.030	0.66	0.20	0.47
DCPIP	+217[d]	1.41	0.029	0.55	0.08	0.52
1,2-naphthoquinone	+143[c]	1.47	0.037	0.48	0.19	0.43
INT	+90[e]	0.76	0.021	0.35	0.11	0.33
PMS	+80[a]	0.74	0.048	0.30	0.42	0.22
thionine	+64[d]	0.46	0.017	0.15	0.11	0.16
NBT	+50[e]	0.22	0.019	0.17	0.10	0.12
methylene blue	+11[d]	0.94	0.035	0.33	0.16	0.22
Meldola blue	−8[d]	1.12	0.113	0.94	0.11	0.70

[a] Ref *49*. [b] Ref *48*. [c] Ref *14*. [d] Ref *50*. [e] Ref *51*.

series of electron acceptors are listed in Table 5. All these protein variants in principle support electron transfer from quinaldine to dioxygen, and to a number of artificial electron acceptors (*48*, *49*). Like wild-type Qox (*4*), mediators with standard potentials E'_0 equal and above −8 mV were used as oxidizing substrates. Indigotetrasulfonate, indigotrisulfonate, indigocarmine, alloxazine, anthraquinone, NAD^+, and methylviologen, with E'_0 of −47, −81, −125, −175, −225, and −450 mV, respectively (*49*−*51*), were not accepted by the Qox variants. Most of the artificial electron acceptors of Qox probably interact with the iron-sulfur centers, as previously suggested for electron transfer from XOR to NBT, $K_3[Fe(CN)_6]$, methylene blue, and PMS (*46*, *52*, *53*). Meldola blue and INT might also accept electrons from FAD, as shown for the flavoprotein 2,4-pentadienoyl-CoA reductase (*54*). DCPIP reduction was previously proposed to occur preferentially at the molybdenum site of XOR (*46*, *53*, *55*). DCPIP, measured under anoxic conditions, was reduced with 2.1−2.2-fold lower activity than dioxygen by most of the Qox proteins listed in Table 5 (Qox_SC60S: 5.6-fold decrease). The specific activity of Qox_SC48S and Qox_SC120S with most oxidizing substrates tested was between 27 and 49% of the activity of Qox with the respective mediator, but NBT and Meldola blue were reduced with higher relative activity. The preparation of Qox_SC40S, which probably has lost the FeSII cluster (see below), showed lowest activities, with 1.9% (O_2) - 10% (Meldola blue) of Qox activity. Even when the specific activities of Qox_SC40S are normalized to its relative iron content (Table 4), its relative activities are only 5−24% of those of Qox. This suggests that FeSII of Qox is the preferred interaction site for most, if not all, mediators.

Reoxidation of the reduced enzyme by dioxygen occurs through the flavin cofactor, so low oxidase activity of Qox proteins carrying cysteine-to-serine substitutions at the [2Fe-2S] centers may reflect a bottleneck of electron transfer at the respective iron of each cluster. When normalizing the specific oxidase activity to the estimated maximal fraction of protein fully occupied with FeS, Qox_SC60S, Qox_SC120S, and Qox_SC48S would show specific oxidase activities of 1.41, 3.91, and 1.93 U/mg, respectively, which correspond to 45, 124, and 61% of Qox oxidase activity (3.14 U/mg). Notably, Qox_SC40S exhibits only 0.15 U per mg of active protein (normalized to its relative iron content of 0.41), i.e., 4.7% of Qox oxidase activity (Table 5). Oxidase activities of Qox_SC45S and Qox_SC154S preparations, which however contained contaminating proteins, were 0.031 U/mg and <0.001 U/mg, respectively.

Taken together, the data on oxidase activity and on activity toward artificial electron acceptors indicate that substitutions at C48, C60, and C120, i.e., at Fe2 of each cluster, do not result in major loss of activity, whereas replacements of the C40 and C154 ligands, i.e., at the Fe1 ions, drastically impede Qox activity.

Substitutions at Fe1 of FeSII: Properties of Qox_SC40S and Qox_SC45S. Consistent with the low overall activity of Qox_SC40S observed with all electron acceptors tested, a substantial decrease in the apparent turnover numbers for both quinaldine and INT was observed for this protein (Table 3). The UV/vis absorption spectrum of Qox_SC40S as isolated and its absorbance ratios (Table 4) suggest a loss in absorbance in the range >420 nm. Addition of an excess of quinaldine to Qox_SC40S resulted in only slight bleaching (Figure 3D).

In line with the UV/vis data, only weak signals of the very rapid Mo(V) species and of FAD were detected by EPR spectroscopy after reduction of Qox_SC40S with quinaldine (Figure 7a, trace A); however, no $[2Fe\text{-}2S]^+$ cluster signals were found at any temperature down to 10 K. Usually, in wild-type Qox as well as in the other Qox proteins discussed, the FeSII signal is always present at low temperatures after reduction with substrate. Reduction with dithionite yielded a spectrum with a typical pattern of FeSI, but again no characteristic FeSII signal could be seen (Figure 7a, trace B). In the case of Qox_SC45S, the reaction with substrate produces very small amounts of the very rapid species and the FAD radical (Figure 7b, trace A) corresponding to its low oxidase activity. No clear indication of an intact FeSII cluster signal is observed, but some rather broad and distorted features (marked with asterisks in Figure 7b, trace B) are found. These have to be taken with some caution, because the background correction procedures of highly accumulated spectra with signals close to the noise level may cause such broad features. However, after reduction with dithionite several EPR signals are recorded, two of which are found close to the *g*-factors of the unperturbed FeSI cluster (Figure 7b, trace C marked with arrows). The typical FeSII-signals are obviously missing, but additional lines, numbered with increasing field, are present. With the available data their assignment is only tentative: Lines 2 and 4 show the same symmetry as the FeSI-signals, but the rather weak shoulder (numbered 5) may also belong to the pattern. Together they

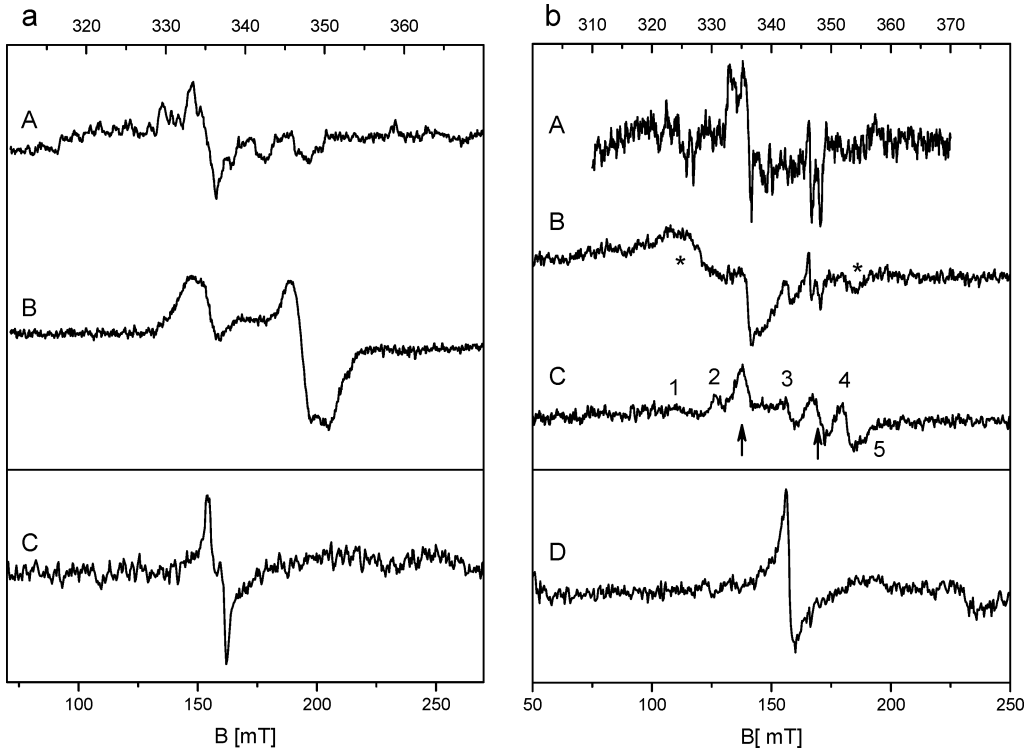

FIGURE 7: EPR spectra of Qox_SC40S (panel a) in the quinaldine- (A, 80 K) and dithionite-reduced (B, 20 K) form. Spectrum C gives the region around $g = 4$ with a Fe^{3+}-signal of the "as isolated" form at 20 K. EPR spectra of Qox_SC45S (panel b) after reduction with substrate at 80 K (A) and 20 K (B) and the dithionite reduced form (20 K, C). The asterisks (in B) mark possible residuals of the subtraction procedure, and the lines with numbers and arrows (in C) are mentioned in the text. Spectrum D (20 K) shows a Fe^{3+}-signal visible in the "as isolated" enzyme.

might represent a strongly modified FeSII center with slight rhombic symmetry (adopted in Table 4). On the other hand, line 2 and 4 could arise from a modified FeSI center with shifted *g*-factors, resulting from the substitution of the cysteine residue C45 that, by analogy to Qor (Figure 1), is located close to residue C152 of FeSI. Finally, the weak lines 1, 3, and possibly 5 may arise from quite small amounts of a residual, slightly modified FeSII center. The relative iron content of Qox_SC40S amounts to about 41% of that of Qox and is even more reduced in Qox_SC45S. This observation is accompanied by the presence of a signal in the low field region of the EPR spectrum around 160 mT, which is a common feature not only of Qox_SC40S and Qox_SC45S (Figure 7, panel a, trace C and panel b, trace D, "as isolated" samples) but also of other variants described below. Typically, this line is not present in recombinant Qox prepared in the same way. This $g = 4.3$ EPR-signal is characteristic of mononuclear $S = 5/2$ Fe^{3+} in a low-symmetry environment and may indicate loss of iron from the clusters in the course of preparation.

For Qox_SC40S the FeSII signal seems to be absent, so that the ratio I/II from reconstruction is 1/0 (Table 4). However, it is possible that there are spectral contributions of low intensity underneath the FeSI-signal, so that FeSII is remaining indistinguishable. In this case, the relative iron content was used as a gross estimate of active enzyme for normalization of the corresponding $k_{cat\ app}$.

These findings show that the serine substitutions at C40 and C45 massively destabilize the FeS-clusters and lead to drastic spectral changes. In particular, the FeSI cluster is severely affected by the replacement of C45 at Fe1 of the FeSII cluster. In the available structures of molybdo-iron/sulfur flavoprotein hydroxylases, the spatial arrangement of the redox centers is highly similar. The distances between the closest iron atoms of the two FeS-clusters vary only between 12.3 and 12.6 Å. The closest ligating cysteines of FeSII and FeSI, which in Qox should correspond to C45 and C152 (cf. Figure 1), approach each other to 5.7−5.9 Å; in Qor, the distance between C53 of FeSII and C142 of FeSI is 5.85 Å. In that respect it is not surprising that the substitution of C45 in Qox_S drastically affected both FeS clusters. Additional experiments and application of other techniques are necessary to clarify the status of the [2Fe-2S] centers in the Qox_SC40S and Qox_SC45S variants.

Substitutions at Fe2 of FeSII: Properties of Qox_SC48S and Qox_SC60S. The iron content of the cluster signals differs drastically between Qox_SC48S and Qox_SC60S (Table 4). The former shows a value close to 1, whereas the latter contains only about 38% of iron relative to Qox, indicating that the C60S substitution destabilizes the [2Fe-2S] clusters. The UV/vis absorption spectrum of Qox_SC48S clearly differed from that of Qox, suggesting a perturbation of the iron-sulfur center(s) in the "as isolated" enzyme (Figure 3E). However, compared with the replacement of C40 at Fe1 of FeSII, the effect of the C60S or C48S substitutions in Qox_S on the apparent k_{cat} values of the enzyme for quinaldine and INT is much less pronounced (Table 3).

In comparison to Qox_SC40S or Qox_SC45S, a different picture is obtained for the Qox_SC48S and Qox_SC60S variants considering their EPR spectra. Reduction of the Qox_SC48S protein with quinaldine resulted in the formation of the very rapid Mo(V) species, the FAD-signal and small contributions of a rapid species visible at high temperature (80 K, Figure 8a, A). At low temperatures (20 K, Figure 8a, trace B) three

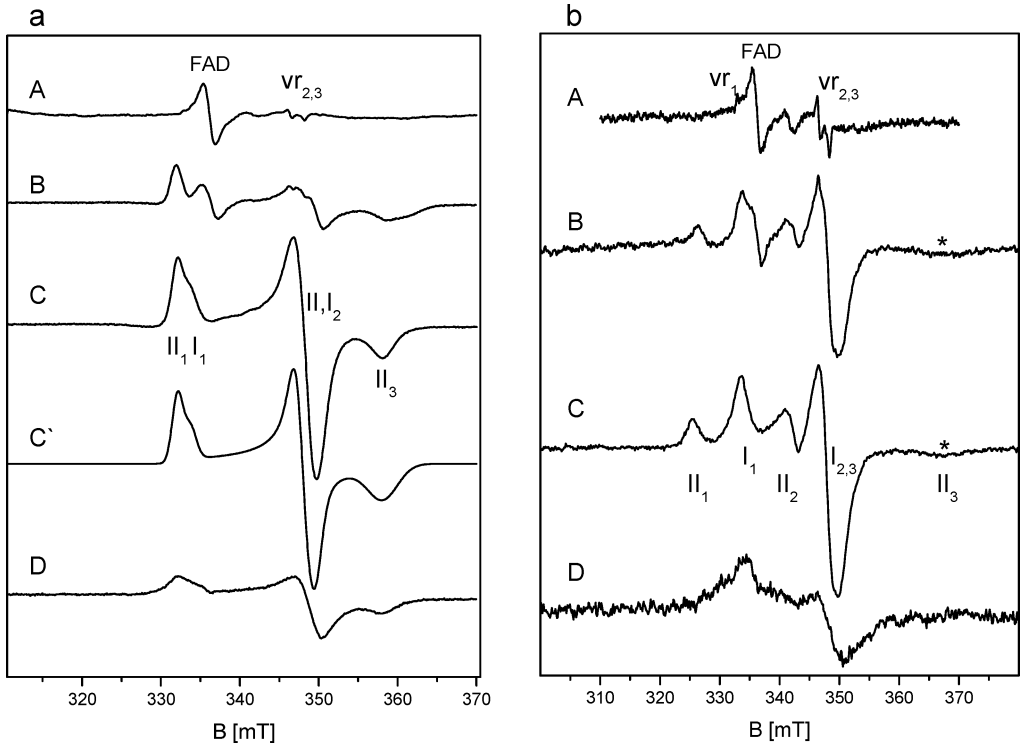

FIGURE 8: EPR spectra of Qox_SC48S (panel a) and Qox_S C60S (panel b) reduced under anoxic conditions with a 20-fold excess of quinaldine (A, B recorded at 80 and 20 K, respectively) and fully reduced with dithionite (C, 20 K). The simulation of the reduced FeSI and FeSII centers of Qox_SC48S is represented in spectrum C′ of panel a. The asterisks in panel b indicate the very broad resonance of the g_3-component of FeSII. Spectra D were recorded at 60 K.

signals of a rhombic [2Fe-2S] center appear whose g_3-component is distorted but corresponds to that of the FeSII-cluster of Qox. Full reduction with dithionite abolished the FAD and Mo(V)-signals revealing a shoulder on the g_1-component of the [2Fe-2S] signals. This spectrum can be simulated with two components, an axial FeSI-signal very similar to the wild-type and a strongly modified rhombic FeSII contribution. For the latter, g_1 approaches the FeSI-signal and g_2 overlaps with the axial signal of FeSI whereas g_3 is similar to that observed in Qox (Figure 8a, traces C and C′, Table 4). A dipolar splitting of the g_1 signal can be excluded by simulations, since the line intensities would show the reversed order (first lower, then higher intensity) with increasing magnetic field. This new FeSII-signal with a much smaller *g*-anisotropy also shows a completely different relaxation behavior with increasing temperature. In Qox, the more rhombic FeSII-signal vanishes above 35 K, but here it is visible up to more than 60 K and is also in this respect more similar to the behavior of FeSI (Figure 8a, trace D). The ratio of FeS-signals I/II from spectral reconstruction yields a lowered content of FeSI contribution (Table 4). However, this ratio should be interpreted cautiously because the spectral contribution of FeSI in the dithionite reduced protein (Figure 8a, trace C) is not really resolved. Hence, other scenarios for spectra simulation, such as a contribution of FeSI to the g_3-component, cannot be excluded. Using the relative iron content of Qox_SC48S alone (≈1) and with the occupation value (2 · 0.3), a range for normalized $k_{cat\ app}$ between 10.6 and 17.7 s^{-1} is estimated (Table 3). This range of the kinetic constant is consistent with the ratio of 0.55 of the FeSII signal intensity in the dithionite and quinaldine reduced sample as compared to Qox (for which a value of 0.7 was determined). The C48 replacement with serine massively affects the electronic structure of the FeSII-center, which becomes apparent via the drastic change of EPR parameters and its relaxation behavior. Because after reduction with quinaldine the new FeSII-signal represents the dominant FeS-species, it is concluded that its redox potential remains clearly higher than that of FeSI as found in the wild-type enzyme. Also the electrons are distributed to all centers (maybe except or with very low concentration to FeSI) showing a behavior similar to Qox.

Addition of quinaldine to the Qox_SC60S variant readily produces the very rapid Mo(V) and FAD EPR signals (Figure 8b, trace A). In contrast to Qox and Qox_SC48S, here signals of both clusters, FeSII and FeSI, are simultaneously visible at low temperature (20 K, Figure 8b, trace B). The EPR spectrum of the dithionite reduced Qox_SC60S yields a pattern that is closely related to the Qox spectrum except for g_3 of FeSII, which shows a very broad resonance (marked with an asterisk) and is shifted to lower *g*-values (1.831 vs 1.877) as shown in Figure 8b, trace C. Apart from that, both [2Fe-2S] centers show a relaxation behavior comparable to recombinant Qox with FeSII vanishing above 35 K (Figure 8b, trace D). The ratio I/II from spectra reconconstruction shows some decrease in the FeSII contribution yielding a normalized $k_{cat\ app}$ approximately half the size of Qox (Table 3). A comparison of signal intensities of both clusters for substrate vs dithionite reduced form yields a factor of about 0.3, which is in line with these data. The simultaneous appearance of both FeS-signals in the presence of substrate can be related to a decreased difference in redox potentials of the [2Fe-2S] clusters in this variant, probably with the FeSII-potential shifted toward that of FeSI (i.e., from −70 mV closer to −250 mV).

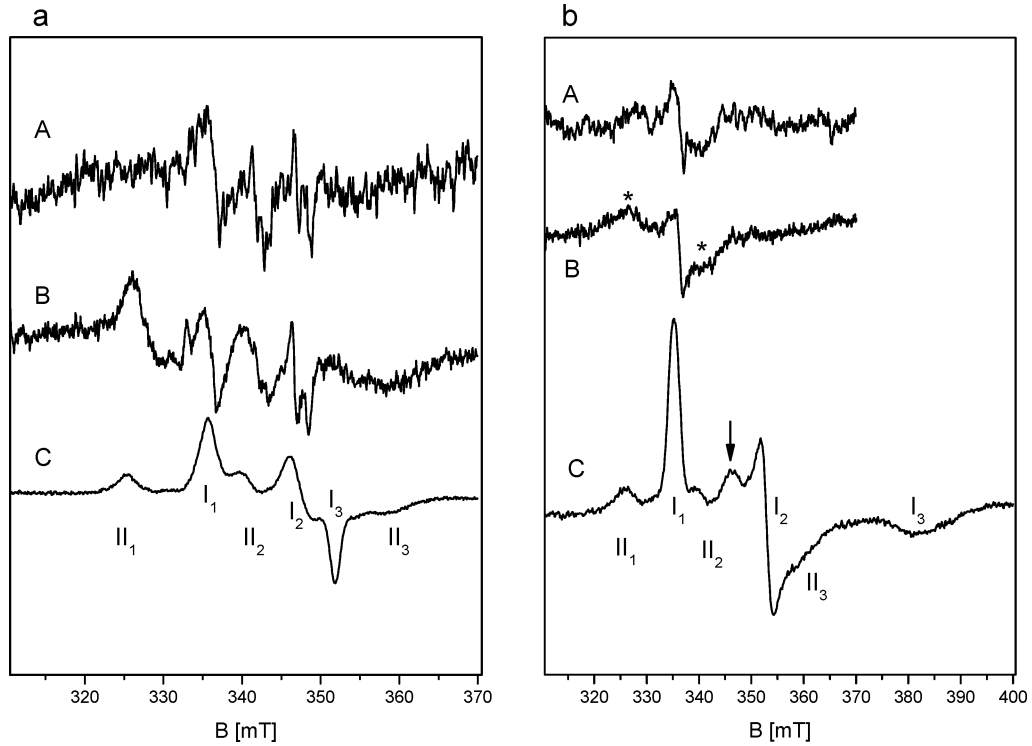

FIGURE 9: EPR signals of Qox_SC120S (panel a) and Qox_SC154S (panel b) observed after anaerobic reduction with quinaldine (A, B) and with dithionite (C). Spectra (A) were recorded at 80 K, spectra (B) and (C) at 20 K. The asterisks mark possible residuals of the background subtraction. The arrow indicates the position of the unperturbed axial FeSI-signal of recombinant Qox.

As shown by EPR spectroscopy and supported by the UV/vis data, electron transfer from the molybdenum center via the [2Fe-2S] centers to FAD (and to the external acceptor dioxygen) is still taking place to a considerable amount in the variants Qox_SC48S and Qox_SC60S. In contrast, serine substitutions at C40 and C45 suppress the characteristic FeSII-signals and nearly abolish catalytic activity. On the whole, the kinetic and spectral properties of the proteins carrying serine substitutions of FeSII cluster ligands may indicate that Fe1, ligated to C40 and C45, is the redox active iron site.

Substitutions at FeSI: Properties of Qox_SC120S and Qox_SC154S. Crystal structures of several molybdenum hydroxylases showed that the Fe1 ion of FeSI is the iron closest to the molybdenum pyranopterin cofactor. In *Oc*CO-DH and *Rc*XDH, for example, it is 5.5 and 5.4 Å from the amino substituent of the pyranopterin ring, respectively (*41*, *42*). Direct contacts between the amino substituent of pyranopterin and S^{γ} of the cysteine ligand which in Qox would correspond to C154 were reported for AORs (*8*, *9*, *40*), bXOR (*10*), *Rc*XDH (*41*), and *Oc*CO-DH (*42*). Qox_SC154S could not be prepared to purity (see above); however, the low specific activity of 0.09 U/mg of the enriched protein (standard INT assay) and especially its negligible oxidase activity (<0.001 U/mg) indicate a severe decrease in the catalytic efficiency of this enzyme.

Residue C120 of Qox_S presumably is a ligand to Fe2 of FeSI (Figure 1). For Qox_SC120S the UV/vis spectrum suggested a decreased absorbance in the 420−500 nm region compared to Qox (Figure 3G; Table 4). Although some loss of [2Fe-2S] is evident from the EPR data (Table 4), the changes in absorption properties may also be governed by effects of the serine substitution on the electronic environment of the [2Fe-2S] center. In contrast to most other Qox variants, the behavior of Qox_SC120S upon reduction with the organic substrate closely resembled that of recombinant Qox. A biphasic kinetic was observed, with about 70% of the enzyme undergoing immediate reduction (considering % of initial absorption at 450 nm), and a second slow phase to reach the endpoint of quinaldine reduction (Figure 3G).

The EPR data show that the [2Fe-2S] centers are assembled in each of the two protein variants; however, a pronounced deviation from axiality typical for the unperturbed FeSI centers is obvious in their corresponding EPR spectra (Figure 9 a,b spectra C). The *g*-factor components of FeSI, particularly g_3 of Qox_SC154S, are drastically different with respect to Qox, but those of FeSII are only slightly modified (Table 4). The relative iron content for the dithionite reduced variants amounts to 0.47 for Qox_SC120S and to about 0.10 to 0.30 for Qox_SC154S, indicating a pronounced destabilization of clusters for the latter variant. Reduction of Qox_SC120S with excess of substrate yields a spectrum constituted of the very rapid species, the flavin semiquinone signal, the signal of the FeSII cluster (Figure 9a, traces A and B) and a small contribution of a Mo(V) resting species already present in the "as isolated" form (not shown). The g_3-component of the FeSII-center is very broad. Similar to Qox, electrons mainly reside on FeSII, FAD and the Mo(V)-cofactor. The ratio of the FeSII signal intensities of substrate- and dithionite-reduced protein amounts to maximally 0.6, showing that this variant has retained considerable activity (the value cannot be determined precisely because the signal in the quinaldine reduced protein is rather distorted). In contrast, when Qox_SC154S is reduced with quinaldine only extremely weak features of the very rapid and FAD signals were detected without any clear indication of the FeSI or FeSII signals (Figure 9b, traces A and B). The broad lines marked with asterisks may be

residuals of the subtraction procedure since they are also present in trace A recorded at 80 K. It is also noted that in the dithionite reduced form a peak marked with an arrow is located exactly in the position of the originally axial FeSI signal (Figure 9 b, trace C), which could arise from a second minority species of FeSI in the Qox_SC154S variant. These EPR results clearly show that for the substitutions at FeSI the clusters are once more destabilized in both cases but in a more drastic way for the Qox_SC154S variant. For a semiquantitative estimate of the spectral contribution of the individual cluster types the spectra were reconstructed, their ratios are given in Table 4. It is evident that the serine substitution at the FeSI center is considerably diminishing the portion of FeSII-signals to about 0.31 for Qox_SC120S and 0.17 for Qox_SC154S. Thus, not only the FeSI center but also the FeSII cluster is strongly influenced by the substitution, which indicates that a disturbed network of residues at the cluster sites may already prevent correct insertion of the [2Fe-2S] clusters.

The normalized $k_{cat\ app}$ value of 9.5 s^{-1} for Qox_SC120S is close to the value found, for example, for Qox_SC60S reflecting decreased but still sizable activity. Thus, the serine substitution at Fe2 (C120S) renders a catalytically competent FeSI center. On the other hand, the protein with the C154S-replacement at Fe1 of FeSI shows very low catalytic activity, practically no Mo(V)- and FeSII EPR signals in the presence of substrate, indicating that the electron transfer is severely impaired. Moreover, pronounced changes in the *g*-value anisotropy and g_{av} value of reduced FeSI center were apparent expanding the spectral range by about 30 mT. Such spectral alterations may be caused by the perturbation of the ligand field at the localized valence Fe(II) site with its intrinsic low-symmetry electronic configuration ($3d^6$), suggesting that Fe1 of FeSI represents the reducible iron site. These observations provide evidence that the Fe1-site is more susceptible to the substitution and therefore may be considered as the reducible iron site, while Fe2 remains in the oxidized state in the FeSI-cluster during turnover. The same reasoning can be applied to FeSII. The proteins with replacements at Fe1 (C40S, C45S) have rather low activities, and no characteristic FeSII signals appear in EPR. In contrast, the serine substitutions at Fe2 (C48S, C60S) leave the enzyme at least with partial activity, and the EPR signals appear in a similar way as in the wild type, suggesting that the Fe2 site of FeSII is less sensitive to the serine substitutions and represents the nonreducible iron site.

Summing up, the results demonstrate that specific substitution of cysteines ligated to the FeS-centers by serine induces a variety of effects. For most variants, a marked loss in iron content is observed, which may be associated with unfavorable folding during assembly of the proteins and/or cluster instability. A low stability of [2Fe-2S] clusters with a serine ligand has also been observed for ferredoxins (*44*, *45*). For rXOR, protein variants carrying serine substitutions of C115 or C51 (which correspond to C120 and C48 of Qox) were reported to be rather unstable, and purification of crude rXOR-C51S preparations was also accompanied by loss of [2Fe-2S] clusters (*18*). Moreover, it appeared that the occupation of the two cluster sites did not merely depend on the substitution at a certain site. Rather, a pronounced mutual influence seems to be present such that a modification of one site strongly affects the population of the other site. The replacement of the cysteine-sulfur by serine-oxygen generally caused specific changes of the spectral EPR pattern usually in both FeS-clusters for the variant proteins, but the most drastic changes were observed for substitutions at the Fe1-iron of the clusters. Finally, the presented results in combination with structural considerations, spectral data on protein variants of rXOR (*56*), and the analysis of intercenter spin−spin interactions in the molybdo-iron/sulfur protein *Dg*AOR (*57*), support the hypothesis that the location of the reducible iron sites of FeSI and FeSII is conserved in proteins of the XO family.

ACKNOWLEDGMENT

We thank Almut Kappius, Münster, for technical assistance.

REFERENCES

1. Overhage, J., Parschat, K., Sielker, S., and Fetzner, S. (2005) Identification of large linear plasmids in *Arthrobacter* spp. encoding or the degradation of quinaldine to anthranilate, *Microbiology 151*, 491−500.
2. Hund, H. K., de Beyer, A., and Lingens, F. (1990) Microbial metabolism of quinoline and related compounds. VI. Degradation of quinaldine by *Arthrobacter* sp., *Biol. Chem. Hoppe-Seyler 371*, 1005−1008.
3. Fetzner, S. (1998) Bacterial degradation of pyridine, indole, quinoline, and their derivatives under different redox conditions, *Appl. Microbiol. Biotechnol. 49*, 237−250.
4. Stephan, I., Tshisuaka, B., Fetzner, S., and Lingens, F. (1996) Quinaldine 4-oxidase from *Arthrobacter* sp. Rü61a, a versatile procaryotic molybdenum-containing hydroxylase active towards N-containing heterocyclic compounds and aromatic aldehydes, *Eur. J. Biochem. 236*, 155−162.
5. Bonin, I., Martins, B. M., Purvanov, V., Fetzner, S., Huber, R., and Dobbek, H. (2004) Active site geometry and substrate recognition of the molybdenum hydroxylase quinoline 2-oxidoreductase, *Structure 12*, 1425−1435.
6. Leimkühler, S., Stockert, A. L., Igarashi, K., Nishino, T., and Hille, R. (2004) The role of active site glutamate residues in catalysis of *Rhodobacter capsulatus* xanthine dehydrogenase, *J. Biol. Chem. 279*, 40437−40444.
7. Huber, R., Hof, P., Duarte, R. O., Moura, J. J. G., Moura, I., Liu, M. Y., LeGall, J., Hille, R., Archer, M., and Romão, M. J. (1996) A structure-based catalytic mechanism for the xanthine oxidase family of molybdenum enzymes, *Proc. Natl. Acad. Sci. U.S.A. 93*, 8846−8851.
8. Rebelo, J., Macieira, S., Dias, J. M., Huber, R., Ascenso, C. S., Rusnak, F., Moura, J. J. G., Moura, I., and Romão, M. J. (2000) Gene sequence and crystal structure of the aldehyde oxidoreductase from *Desulfovibrio desulfuricans* ATCC 27774, *J. Mol. Biol. 297*, 135−146.
9. Rebelo, J. M., Dias, J. M., Huber, R., Moura, J. J. G., and Romão, M. J. (2001) Structure refinement of the aldehyde oxidoreductase from *Desulfovibrio gigas* (MOP) at 1.28 Å, *J. Biol. Inorg. Chem. 6*, 791−800.
10. Enroth, C., Eger, B. T., Okamoto, K., Nishino, T., Nishino, T., and Pai, E. F. (2000) Crystal structures of bovine milk xanthine dehydrogenase and xanthine oxidase: structure-based mechanism of conversion, *Proc. Natl. Acad. Sci. U.S.A. 97*, 10723−10728.
11. Canne, C., Stephan, I., Finsterbusch, J., Lingens, F., Kappl, R., Fetzner, S., and Hüttermann, J. (1997) Comparative EPR and redox studies of three prokaryotic enzymes of the xanthine oxidase family: quinoline 2-oxidoreductase, quinaldine 4-oxidase, and isoquinoline 1-oxidoreductase, *Biochemistry 36*, 9780−9790.
12. Canne, C., Lowe, D. J., Fetzner, S., Adams, B., Smith, A. T., Kappl, R., Bray, R. C., and Hüttermann, J. (1999) Kinetics and interactions of molybdenum and iron-sulfur centers in bacterial enzymes of the xanthine oxidase family: mechanistic implications, *Biochemistry 38*, 14077−14087.
13. Lowe, D. J., and Bray, R. C. (1978) Magnetic coupling of the molybdenum and iron-sulphur centres in xanthine oxidase and xanthine dehydrogenases, *Biochem. J. 169*, 471−479.

14. Barber, M. J., Salerno, J. C., and Siegel, L. M. (1982) Magnetic interactions in milk xanthine oxidase, *Biochemistry 21*, 1648−1656.
15. Kappl, R., Hüttermann, J., and Fetzner, S. (2002) The molybdenum-containing hydroxylases of quinoline, isoquinoline and quinaldine, in *Molybdenum and Tungsten: Their Roles in Biological Processes* (Sigel, A., and Sigel, H., Eds.) Vol. 39, pp 481−537, Marcel Decker, New York.
16. Caldeira, J., Belle, V., Asso, M., Guigliarelli, B., Moura, I., Moura, J. J. G., and Bertrand, P. (2000) Analysis of the electron paramagnetic resonance properties of the $[2Fe\text{-}2S]^{1+}$ centers in molybdenum enzymes of the xanthine oxidase family: Assignment of signals I and II, *Biochemistry 39*, 2700−2707.
17. Andrade, S. L. A., Brondino, C. D., Feio, M. J., Moura, I., and Moura, J. J. G. (2000) Aldehyde oxidoreductase activity in *Desulfovibrio alaskensis* NCIMB 13491. EPR assignment of the proximal [2Fe-2S] cluster to the Mo site, *Eur. J. Biochem. 267*, 2054−2061.
18. Iwasaki, T., Okamoto, K., Nishino, T., Mizushima, J., and Hori, H. (2000) Sequence motif-specific assignment of two [2Fe-2S] clusters in rat xanthine oxidoreductase studied by site-directed mutagenesis, *J. Biochem. (Tokyo) 127*, 771−778.
19. Parschat, K., Hauer, B., Kappl, R., Kraft, R., Hüttermann, J., and Fetzner, S. (2003) Gene cluster of *Arthrobacter ilicis* Rü61a involved in the degradation of quinaldine to anthranilate. Characterization and functional expression of the quinaldine 4-oxidase *qoxLMS* genes, *J. Biol. Chem. 278*, 27483−27494.
20. Werth, M. T., Cecchini, G., Manodori, A., Ackrell, B. A. C., Schröder, I., Gunsalus, R. P., and Johnson, M. K. (1990) Site-directed mutagenesis of conserved cysteine residues in *Escherichia coli* fumarate reductase: Modification of the spectroscopic and electrochemical properties of the [2Fe-2S] cluster, *Proc. Natl. Acad. Sci. U.S.A. 87*, 8965−8969.
21. Xia, B., Cheng, H., Bandarian, V., Reed, G. H., and Markley, J. L. (1996) Human ferredoxin: Overproduction in *Escherichia coli*, reconstitution *in vitro*, and spectroscopic studies of iron-sulfur cluster ligand cysteine-to-serine mutants, *Biochemistry 35*, 9488−9495.
22. Bagdasarian, M., Lurz, R., Rückert, B., Franklin, F. C., Bagdasarian, M. M., Frey, J., and Timmis, K. N. (1981) Specific-purpose plasmid cloning vectors. II. Broad host range, high copy number, RSF1010-derived vectors, and a host-vector system for gene cloning in *Pseudomonas*, *Gene 16*, 237−247.
23. Nelson, K. E., Weinel, C., Paulsen, I. T., Dodson, R. J., Hilbert, H., Martins dos Santos, V. A. P., Fouts, D. E., Gill, S. R., Pop, M., Holmes, M., Brinkac, L., Beanan, M., DeBoy, R. T., Daugherty, S., Kolonay, J., Madupu, R., Nelson, W., White, O., Peterson, J., Khouri, H., Hance, I., Chris Lee, P., Holtzapple, E., Scanlan, D., Tran, K., Moazzez, A., Utterback, T., Rizzo, M., Lee, K., Kosack, D., Moestl, D., Wedler, H., Lauber, J., Stjepandic, D., Hoheisel, J., Straetz, M., Heim, S., Kiewitz, C., Eisen, J., Timmis, K. N., Düsterhöft, A., Tümmler, B., and Fraser, C. M. (2002) Complete genome sequence and comparative analysis of the metabolically versatile *Pseudomonas putida* KT2440, *Environ. Microbiol. 4*, 799−808.
24. Blatny, J. M., Brautaset, T., Winther-Larsen, H. C., Haugan, K., and Valla, S. (1997) Construction and use of a versatile set of broad-host-range cloning and expression vectors based on the RK2 replicon, *Appl. Environ. Microbiol. 63*, 370−379.
25. Vieira, J., and Messing, J. (1982) The pUC plasmids, an M13mp7-derived system for insertion mutagenesis and sequencing with synthetic universal primers, *Gene 19*, 259−268.
26. Grant, S. G. N., Jessee, J., Bloom, F. R., and Hanahan, D. (1990) Differential plasmid rescue from transgenic mouse DNAs into *Escherichia coli* methylation-restriction mutants, *Proc. Natl. Acad. Sci. U.S.A. 87*, 4645−4649.
27. Sambrook, J., Fritsch, E. F., and Maniatis, T. (1989) *Molecular Cloning: A Laboratory Manual*. Cold Spring Laboratory Press: Cold Spring Harbor, New York.
28. Tshisuaka, B., Kappl, R., Hüttermann, J., and Lingens, F. (1993) Quinoline oxidoreductase from *Pseudomonas putida* 86: an improved purification procedure and electron paramagnetic resonance spectroscopy, *Biochemistry 32*, 12928−12934.
29. Babson, A. L., and Babson, S. R. (1973) Kinetic colorimetric measurement of serum lactate dehydrogenase activity, *Clin. Chem. 19*, 766−769.
30. Schellenberg, K. A., and Hellerman, L. (1958) Oxidation of reduced diphosphopyridine nucleotide, *J. Biol. Chem. 231*, 547−556.
31. Armstrong, J. M. (1964) The molar extinction coefficient of 2,6-dichlorophenol indophenol, *Biochim. Biophys. Acta 86*, 194−197.
32. Dixon, M. (1971) The acceptor specificity of flavins and flavoproteins. II. Free flavins, *Biochim. Biophys. Acta 226*, 259−268.
33. Roerig, D. L., Mascaro, L., Jr., and Aust, S. D. (1972) Microsomal electron transport: tetrazolium reduction by rat liver microsomal NADPH-cytochrome c reductase, *Arch. Biochem. Biophys. 153*, 475−479.
34. Lehmann, M., Tshisuaka, B., Fetzner, S., Röger, P., and Lingens, F. (1994) Purification and characterization of isoquinoline 1-oxidoreductase from *Pseudomonas diminuta* 7, a novel molybdenum-containing hydroxylase, *J. Biol. Chem. 269*, 11254−11260.
35. Lowry, O. H., Rosebrough, N. J., Farr, A. L., and Randall, R. J. (1951) Protein measurement with the Folin phenol reagent, *J. Biol. Chem. 193*, 265−275.
36. Laemmli, U. K. (1970) Cleavage of structural proteins during the assembly of the head of bacteriophage T4, *Nature 227*, 680−685.
37. Olson, J. S., Ballou, D. P., Palmer, G., and Massey, V. (1974) The mechanism of action of xanthine oxidase, *J. Biol. Chem. 249*, 4363−4382.
38. Romão, M. J., and Huber, R. (1998) Structure and function of the xanthine-oxidase family of molybdenum enzymes, *Struct. Bonding (Berlin) 90*, 69−95.
39. Okamoto, K., Matsumoto, K., Hille, R., Eger, B. T., Pai, E. F., and Nishino, T. (2004) The crystal structure of xanthine oxidoreductase during catalysis: Implications for reaction mechanism and enzyme inhibition, *Proc. Natl. Acad. Sci. U.S.A. 101*, 7931−7936.
40. Romão, M. J., Archer, M., Moura, I., Moura, J. J. G., LeGall, J., Engh, R., Schneider, M., Hof, P., and Huber, R. (1995) Crystal structure of the xanthine oxidase-related aldehyde oxido-reductase from *D. gigas*, *Science 270*, 1170−1176.
41. Truglio, J. J., Theis, K., Leimkühler, S., Rappa, R., Rajagopalan, K. V., and Kisker, C. (2002) Crystal structures of the active and alloxanthine-inhibited forms of xanthine dehydrogenase from *Rhodobacter capsulatus*, *Structure 10*, 115−125.
42. Dobbek, H., Gremer, L., Meyer, O., and Huber, R. (1999) Crystal structure and mechanism of CO dehydrogenase, a molybdo iron-sulfur flavoprotein containing S-selanylcysteine, *Proc. Natl. Acad. Sci. U.S.A. 96*, 8884−8889.
43. Fujinaga, J., Gaillard, J., and Meyer, J. (1993) Mutated forms of a [2Fe-2S] ferredoxin with serine ligands to the iron-sulfur cluster, *Biochem. Biophys. Res. Commun. 194*, 104−111.
44. Meyer, J., Fujinaga, J., Gaillard, J., and Lutz, M. (1994) Mutated forms of the [2Fe-2S] ferredoxin from *Clostridium pasteurianum* with noncysteinyl ligands to the iron-sulfur cluster, *Biochemistry 33*, 13642−13650.
45. Cheng, H., Xia, B., Reed, G. H., and Markley, J. L. (1994) Optical, EPR, and ^{1}H NMR spectroscopy of serine-ligated [2Fe-2S] ferredoxins produced by site-directed mutagenesis of cysteine residues in recombinant *Anabaena* 7120 vegetative ferredoxin, *Biochemistry 33*, 3155−3164.
46. Coughlan, M. P. (1980) Aldehyde oxidase, xanthine oxidase and xanthine dehydrogenase: hydroxylases containing molybdenum, iron-sulphur and flavin, in *Molybdenum and Molybdenum-containing Enzymes* (Coughlan, M.P., Ed.) pp 119−185, Pergamon Press, Oxford.
47. Komai, H., Massey, V., and Palmer, G. (1969) The preparation and properties of deflavo xanthine oxidase, *J. Biol. Chem. 244*, 1692−1700.
48. Loach, P. A. (1976) Oxidation-reduction potentials, absorbance bands and molar absorbance of compounds used in biochemical studies, in *Handbook of Biochemistry and Molecular Biology* (Fasman, G. D., Ed.) 3rd ed., pp 122−130, CRC Press, London.
49. Peel, J. L. (1972) The use of electron acceptors, donors and carriers, *Methods Microbiol. 6B*, 1−24.
50. Günther, H., and Simon, H. (1995) Artificial electron carriers for preparative biocatalytic redox reactions forming reversibly carbon hydrogen bonds with enzymes present in strict or facultative anaerobes, *Biocatal. Biotransform. 12*, 1−26.

51. Michal, G., Möllering, H., and Siedel, J. (1983) Chemical Design of Indicator Reaction for the Visible Range, in *Methods of Enzymatic Analysis* (Bergmeyer, H. U., Bergmeyer, J., Graβl, M., Eds.) Vol. 1, pp 197−232, Verlag Chemie, Weinheim.
52. Kelner, M. J., Bagnell, R., Hale, B., and Alexander, N. M. (1988) Methylene blue competes with paraquat for reduction by flavoenzymes resulting in decreased superoxide production in the presence of heme proteins, *Arch. Biochem. Biophys. 262*, 422−426.
53. Hughes, R. K., Doyle, W. A., Chovnick, A., Whittle, J. R., Burke, J. F., and Bray, R. C. (1992) Use of rosy mutant strains of *Drosophila melanogaster* to probe the structure and function of xanthine dehydrogenase, *Biochem. J. 285*, 507−513.
54. Eikmanns, U., and Buckel, W. (1991) A green 2,4-pentadienoyl-CoA reductase from *Clostridium aminovalericum*, *Eur. J. Biochem. 198*, 263−266.
55. Gurtoo, H. L., and Johns, D. G. (1971) On the interaction of the electron acceptor 2,6-dichlorophenolindophenol with bovine milk xanthine oxidase, *J. Biol. Chem. 246*, 286−293.
56. Nishino, T., and Okamoto, K. (2000) The role of the [2Fe-2S] cluster centers in xanthine oxidoreductase, *J. Inorg. Biochem. 82*, 43−49.
57. More, C., Asso, M., Roger, G., Guigliarelli, B., Caldera, J., Moura, J., and Bertrand, P. (2005) Study of the spin-spin interactions between the metal centers of *Desulfovibrio gigas* aldehyde oxidoreductase: identification of the reducible sites of the [2Fe-2S]$^{1+,2+}$ clusters, *Biochemistry 44*, 11628−11635.

BI061185A